Chemical Engineering Journal 204–206 (2012) 32–39

Contents lists available at SciVerse ScienceDirect

Chemical Engineering Journal

journal homepage: www.elsevier.com/locate/cej

Degradation of azo dye using non-thermal plasma advanced oxidation process in a circulatory airtight reactor system

Bo Jiang, Jingtang Zheng *, Qian Liu, Mingbo Wu *

State Key Laboratory of Heavy Oil Processing, China University of Petroleum, Dongying 257061, Shandong, PR China

HIGHLIGHTS

- Design of a circulatory airtight non-thermal plasma reactor for the removal of azo dye.
- The effects of various electrical and chemical parameters were studied.
- Comparison of degradation efficiency between various non-thermal plasma reactor.
- Bond dissociation energies (BDEs) theory is applied for proposing degradation mechanism.

GRAPHICAL ABSTRACT

The degradation of methyl orange could be increased significantly in the circulatory airtight non-thermal plasma reactor.

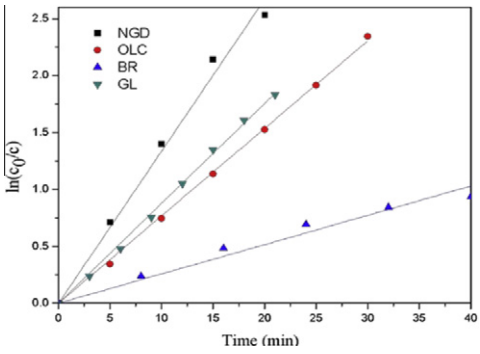

ARTICLE INFO

Article history:
Received 30 March 2012
Received in revised form 4 July 2012
Accepted 18 July 2012
Available online 28 July 2012

Keywords:
Methyl orange
Degradation
Non-thermal plasma
Circulatory airtight reactor system

ABSTRACT

To improve the energy efficiency in dye degradation, a circulatory airtight reactor system was developed. Experiments were conducted to estimate the effects of various parameters on the degradation of methyl orange (MO). It was found that MO degradation depended on the initial concentration and total volume of the compound, being slower for higher concentrations and larger volumes. There existed a maximal MO decoloration efficiency with the change of oxygen velocity. This reactor had better performance of the conductivity resistance on MO degradation. Relatively high or low pH of the solution was adverse for MO removal. After 20 min plasma treatment, 92% removal of MO was achieved and the corresponding energy efficiency was 11.68 g/kW h with gas velocity of 0.08 m^3/h and the input energy of 5.67 W. Besides, compared with three other reactor systems, this gas discharge reactor system expressed prominent energy efficiency and supreme reaction rate constant. Lastly, bond dissociation energies (BDEs) theory was applied to propose the degradation mechanism of MO.

1. Introduction

The wastewaters generated by the textile industry contain considerable amounts of azo dyes. Many dyes are toxic, biologically rather resistant and apt to cause genetic mutations, which cannot be recognized and degraded easily by the natural environment [1,2]. Therefore, development of effective wastewater treatment technologies is one of the most critical and urgent tasks for researchers.

Considerable attention has been paid to so-called advanced oxidation processes (AOPs), such as Photocatalysis [3], Fenton processes [4], and UV/H_2O_2 [5], based on in situ generation of strong oxygen-based oxidizers, especially hydroxyl radical, which is among the strongest oxidizers and reacts non-selectively with

* Corresponding authors. Tel.: +86 13854628317; fax: +86 546 8395190.
E-mail addresses: jtzheng03@163.com (J. Zheng), wmbpeter@yahoo.com (M. Wu).

1385-8947/$ - see front matter © 2012 Elsevier B.V. All rights reserved.
http://dx.doi.org/10.1016/j.cej.2012.07.088

various types of pollutants [6]. The non-thermal plasma technology, as one of the AOPs, leads to various physical and chemical effects, such as pyrolysis, UV photolysis, electrohydraulic cavitation, as well as formation of oxidizing species: radicals ($H^{\cdot}$,$O^{\cdot}$,$OH^{\cdot}$) and molecules (H_2O_2, O_3, etc.) [7,8]. This technology utilized in wastewater treatment attracts particular interest due to its excellent performance of attacking organic pollutant and having no secondary pollution [6,8].

As a typical electrical discharge model, compared with liquid discharge, gas discharge owns many advantages such as more active species generated, lower discharge inception voltage as well as larger discharge zone [9,10]. However, the plasma species can only reach the substrate by diffusion, and the formed oxide layer is generally thin, typically less than 10 nm in gas discharge process [11]. So the efficiency of this process generally suffers from gas–liquid interphase mass transfer resistance, which greatly limits the application of this discharge system. In order to improve the pollutant degradation efficiency, a flowing film reactor has been designed and studied for either liquid-phase or gas-phase treatment [6,12]. Nevertheless, the energy efficiency has limited improvement. There is yet great space of improvement with designing more effective reactor system.

In the present work, a gas discharge circulatory airtight reactor system (GDC) was developed over needles–plate electrode system and methyl orange (MO) was selected as a model pollutant dye. Experimental measurements were carried out to determine the effect of initial concentration, total volume, gas velocity, solution conductivity and solution pH on decoloration efficiency of the dye. Besides, the concentrations of hydrogen peroxide and ozone produced in different conditions were determined. At last, this study compared the efficacy of four different reactor systems for MO degradation.

2. Experimental

2.1. Materials and reaction system

All chemicals used in this study were purchased from Sinopharm Chemical Reagent Co., Ltd., Shanghai, China and their CAS numbers are given in Table S1 (Supporting Information). Distilled water with conductivity of less than 5 μS/cm was used to prepare all solutions.

The experimental apparatus consisted of a pulse power supply and a non-thermal plasma-based water treatment reactor system (Fig. 1a and b). Voltage and pulse repetition rate range of the pulse power supply (DMG-60) were 0–60 kV and 0–320 pulses per second (pps), respectively. Output capacitance was 67 pF and pulse rise time was less than 100 ns. And the reactor was mainly made up of high voltage pin-electrodes, stainless steel ground electrode, rubber tube, peristaltic pump (ATP-3200), sampling pipe and two plexiglas cylinders ($Ø_{(reactor)}$ = 65 mm, $Ø_{(reservoir)}$ = 30 mm) connected in series. The high-voltage electrode (discharging electrode) was vertically placed above the surface of the liquid. The distance between the needles electrode and water surface can be adjusted, and 5 mm distance was selected to minimize the sparking voltage within the reactor. The ground electrode was submerged in the liquid with a distance of 15 mm under gas–liquid interface. The details of needles electrode and ground electrode were depicted in Fig. 1c. MO solution was pumped into reactor by a peristaltic pump at 60 mL/min, flew as a film on the upside of the earthed electrode and finally returned to the solution reservoir. Oxygen gas was compressed into the reactor through an air inlet tube, and passed by a side of the ground electrode into the discharge region. After passing through the discharge zone, plasma gas existed through the tube with the liquid and bubbled through the liquid in the reservoir.

2.2. Experimental methods and analysis

Hydrochloric acid and sodium hydroxide were used to adjust solution pH value. Sodium chloride was used to modify solution conductivity. The conductivity and pH of the solution were measured by conductivity meter (DDS-11A) and pH meter (pHSJ-3F), respectively. The production of hydrogen peroxide in aqueous solution was determined colorimetrically using reaction of H_2O_2 with titanyl ions [13]. The concentration of dissolved ozone was determined by the Indigo method [14]. The concentrations of MO solution were calculated by measuring the absorbencies of the solution at 465 nm wavelength using Hach DR-2500 Spectrophotometer. The chemical oxygen demand (COD) was measured with a CM-02 COD analyzer (Beijing Shuanghui Corp., China). NO_3^- and SO_4^{2-} were detected using Ion chromatography (ICS-3000). All experiments were conducted in triplicate at the input power of 5.67 W (46 kV, 80 pps) and gave reproducibility of within 5%. Typically, 2 mL samples were taken from the reactor vessel at fixed intervals during each run.

The decoloration efficiency η can be calculated as:

$$\eta\ (\%) = \frac{C_0 - C}{C_0} \times 100 \tag{1}$$

where C_0 and C are the initial and the final concentration of MO solution, respectively.

The COD removal was calculated using the following equation:

$$\mathrm{COD}\ (\%) = \frac{\mathrm{COD}_0 - \mathrm{COD}}{\mathrm{COD}_0} \times 100 \tag{2}$$

where COD_0 is the chemical oxygen demand of initial solution and COD is the chemical oxygen demand at time t.

MO removal rates could be described by first-order kinetics with good correlation coefficient values (>0.96):

$$Ln\left(\frac{C}{C_0}\right) = -kt \tag{3}$$

The efficiency of MO degradation, the dissolved O_3 and H_2O_2 generated was illustrated by the energy yield and defined as follows:

$$G(\mathrm{MO})\ [\mathrm{g/kW\,h}] = \frac{C_0 V \eta(\%)}{100Pt} \tag{4}$$

$$G(\mathrm{O_3})\ [\mathrm{g/kW\,h}] = \frac{C_{O_3} V}{Pt} \tag{5}$$

$$G(\mathrm{H_2O_2})\ [\mathrm{g/kW\,h}] = \frac{C_{H_2O_2} V}{Pt} \tag{6}$$

C_{O_3} and $C_{H_2O_2}$ are the concentrations of O_3 and H_2O_2, respectively at the end of treatment. V is total solution volume. P is input power and t is discharge time.

3. Results and discussion

3.1. Effect of initial concentrations and total volumes on MO degradation

The decoloration efficiency (η) as a function of treatment time is presented in Fig. 2a. It is seen that η decreased with the increase of initial solution concentration and the total volumes. For example, after 20 min plasma treatment, the decoloration efficiency was 95.6% for 300 mL MO solution and reduced to 87.6% for 600 mL. Since under steady discharge, the active species produced in pulse discharge were maintained at specific concentration levels leading to a maximum degradation capability. Fig. 2b compares the energy yield (G_{MO}) as a function of η with different initial solution

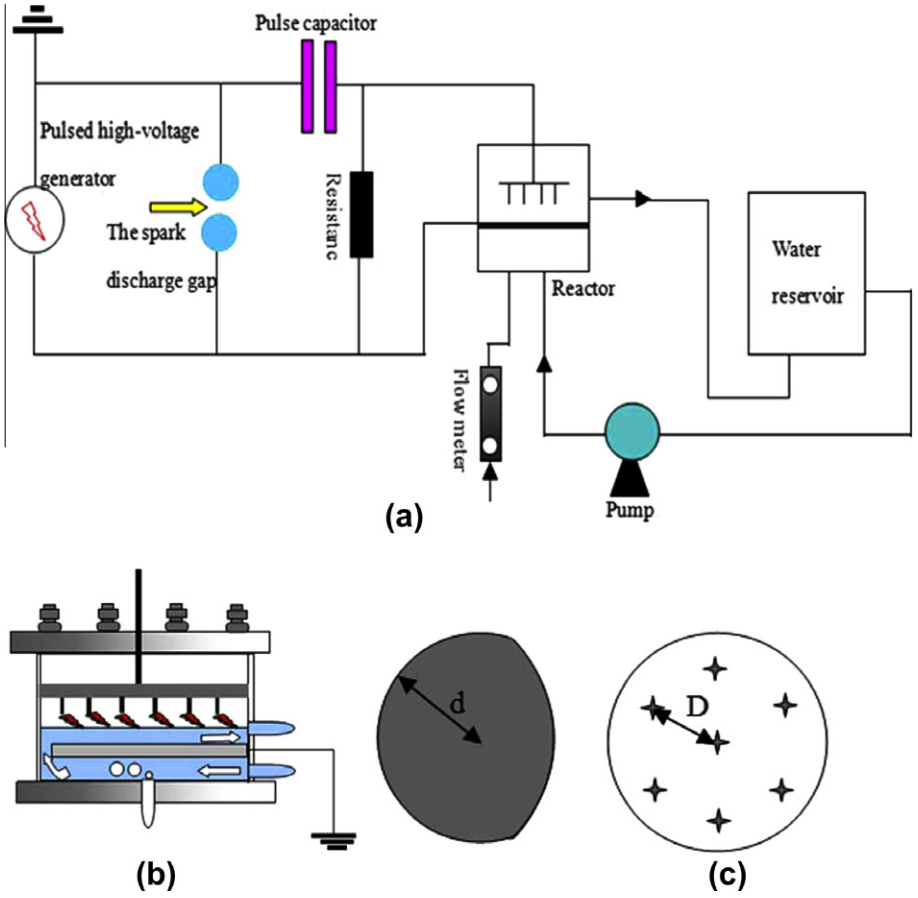

Fig. 1. (a) Detailed schematic of a circulatory airtight reactor, (b) needles electrode, and (c) ground electrode (d = 31 mm – radius of ground electrode; D = 15 mm – needle spacing).

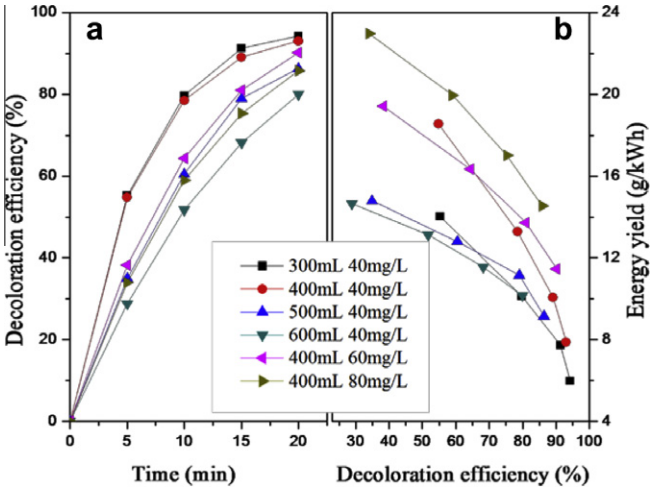

Fig. 2. Effect of initial concentrations on MO degradation (conditions: input energy 5.67 W; gas flow rate 0.06 m^3/h; treatment time 20 min; temperature: 283 K).

concentrations and the total volumes. For the initial 5 min of plasma treatment, G_{MO} increased but η decreased with increasing the initial concentration of MO. Fig. 2b also shows that G_{MO} reduced significantly with treatment time extending due to less dye molecules residual in liquid for decomposition.

Table S2 (Supporting Information) shows decoloration efficiency and energy yield of MO using non-thermal plasma technology with different plasma reactors. The obtained result presents that gas discharge in GDC was capable of removing up to 92% of MO in 20 min corresponding to a removal yield of 11.68 g/kW h. In GDC process, the plasma originating from the high-voltage electrode directly attacked the MO molecules and decomposed water molecules into hydroxyl radicals which then destructed the bonds of organic in gas–liquid interface zone. At the same time, there is always fresh solution exposure to plasma due to liquid circulating, which compensated mass transfer resistance to some extent. Besides, large number of reactive gas species not diffusing into the liquid flew into the reservoir with secondary comprehensive utilization. Thus, compared with these previous reactor systems, higher decoloration efficiency and better energy efficiency can be both obtained with lower energy input in GDC.

As compared with AOPs, some conventional approaches, such as biological treatment [15], ultrafiltration [16,17], adsorption [18,19] coagulation–flocculation [20], are non-destructive or slow rates of destruction. For example, biological degradation requires high reaction volume as well as long treatment time and high specificity. Some other AOPs were also used for dyes degradation besides plasma technology, e.g. Photocatalytic oxidation [3], Wet oxidation [21], Radiolysis [22], Fenton processes [4], UV/H_2O_2 [5], UV/Fenton [23], etc. These technology need radiation sources or chemicals addition, which are high energy consumption and environmentally hazardous. For example, for the decomposition of MO (solution volume: 80 mL, initial concentration 5 mg/L) by nanocrystalline mesoporous-assembled TiO_2 photocatalysis, Jantawasu et al. [3] used a low-pressure mercury lamp and obtained about 78% conversion after 4 h treatment. The energy cost was rather high as compared to non-thermal plasma, where the power involved was

3 orders of magnitude lower. As compared to other common AOPs, the primary benefit of plasma is the ability to generate UV light and oxidizing species, ozone, hydroxyl radicals, etc. without chemical addition or the use of UV lamps [7,8].

3.2. Effect of gas velocity

Various gas velocities were applied to study their effects on the degradation of MO. As shown in Fig. 3, it is observed that increasing the gas velocity from 0.02 m^3/h to 0.12 m^3/h improved the degradation of MO with treatment time of 20 min. The highest decoloration efficiency of MO reached 93.7% at a gas velocity of 0.12 m^3/h, which was about 6.4% more than the decoloration efficiency obtained at a gas velocity of 0.02 m^3/h. The possible explanation for this phenomenon is that the destruction of ozone may happen and reduce the mass flux of ozone downstream in the plasma region at low gas velocities with fixed energy input [24]. This perspective can be validated by the experiment data that more O_3 was generated with the increase of gas velocity at a fixed energy input in Fig. 4. With the increase of gas velocity, more gas molecules passed through the discharge zone and were broken down by energetic electrons within the same time span, and hence more reactive species were generated resulting in more degradation reactions [25]. On the other hand, larger flow rate led to turbulent flow of liquid, which made reaction more intensive in the interface and more active gas diffuse into the liquid. However with the further increase of gas velocity over 0.12 m^3/h, the residence time of gas in reservoir was shortened, accordingly, the utilization efficiency of reactive species was decreased. Therefore, the decoloration efficiency for gas velocity of 0.14 m^3/h began to reduce. Fig. 4 presents that compared with that in MO solution, the yield of O_3 significantly reduced after 20 min plasma treatment in distilled water with the velocity of 0.06 m^3/h. And it can be concluded that compared with H_2O_2, O_3 denoted more important for MO degradation due to its relative high oxidation potential.

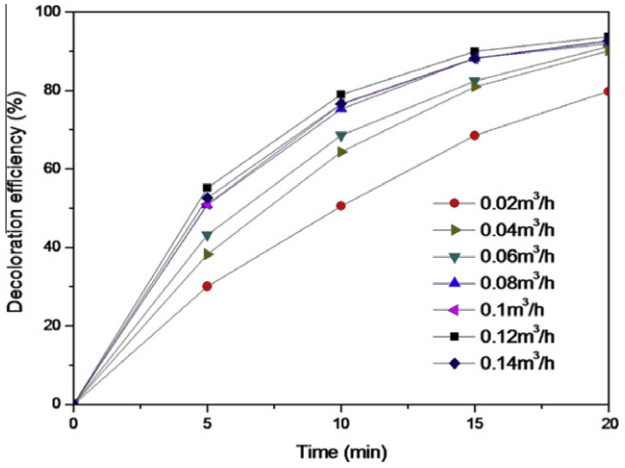

Fig. 3. Effect of gas velocities on MO degradation (conditions: input energy 5.67 W; total volume 400 mL; initial concentration 60 mg/L; treatment time 20 min; temperature: 283 K).

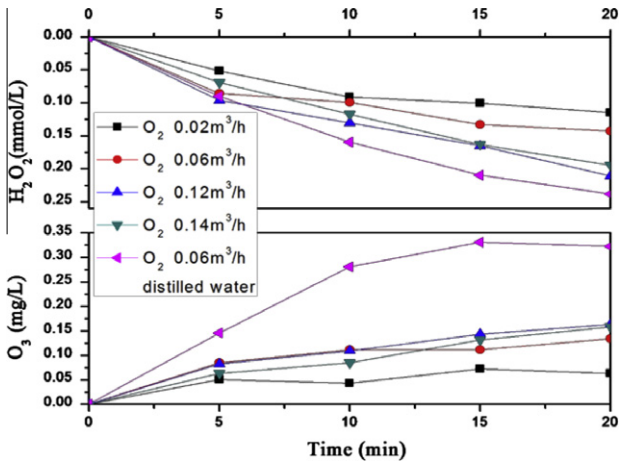

Fig. 4. Effect of gas velocities on concentrations of H_2O_2 and O_3 (conditions: input energy 5.67 W; total volume 400 mL; initial concentration 60 mg/L; treatment time 20 min; temperature: 283 K).

In the plasma reaction, a large amount of atomic oxygen can be formed through electron impact dissociation of oxygen, which resulted in a larger generation of ozone. H_2O_2 can also be produced with electron dissociating H_2O after a series of reactions. At the same time, generated O_3 and H_2O_2 were decomposed by some elections and radials and consumed for organic degradation. Thus, the formation and consumption of ozone and hydrogen peroxide appeared synchronously. Related formulas describing the generation reactions of O_3 and H_2O_2 were exhibited as follows [7,24]:

$$e^- + O_2 \rightarrow O + O + e^- \quad (7)$$

$$O + O_2 \rightarrow O_3 \quad (8)$$

$$e^- + O_2 \rightarrow O_2^* + e^- \quad (9)$$

$$O_2^* + O_2 \rightarrow O_3 + O \quad (10)$$

$$e^- + O_3 \rightarrow O + O_2 + e^- \quad (11)$$

$$e^- + H_2O \rightarrow OH^\cdot + H^\cdot \quad (12)$$

$$OH^\cdot + OH^\cdot \rightarrow H_2O_2 \quad (13)$$

$$O + H_2O \rightarrow OH^\cdot + OH^\cdot \quad (14)$$

$$H_2O_2 + OH^\cdot \rightarrow H_2O + HO_2^\cdot \quad (15)$$

3.3. Effect of conductivity

Initial solution conductivity is an important factor that affects the decoloration efficiency of the plasma processes [26]. In this

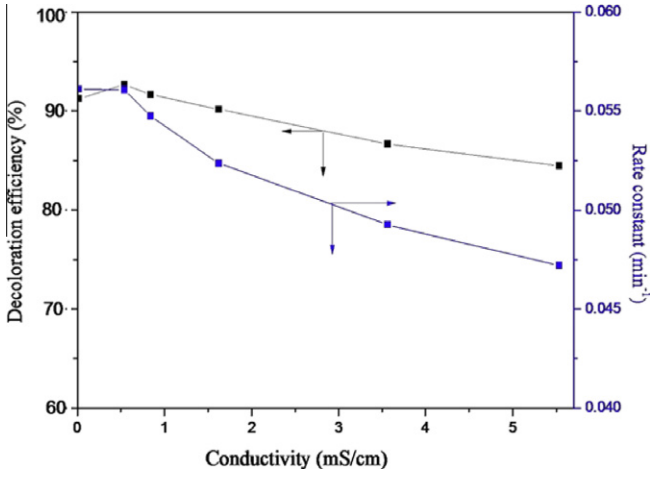

Fig. 5. Effect of conductivities on MO degradation (conditions: input energy 5.67 W; total volume 400 mL; initial concentration 60 mg/L; gas velocity rate 0.06 m^3/h; treatment time 20 min; virgin conductivity 17.4 μS/cm; temperature: 283 K).

system, with increasing the conductivity, the decoloration efficiency and rate constant both had descending trend (see Fig. 5). For example, the rate constant for virgin solution was 0.05612 min^{-1} and it was only 0.04721 min^{-1} for the solution with conductivity of 5.53 mS/cm. The possible reason is that higher conductivity led to larger discharge current, more intensive UV light and stronger acoustic waves. Compared with contribution of active radials for organic degradation, these physical phenomena expressed less importance for organic degradation but favored heating of solution [8]. And stronger physical phenomenon consumed more energy with increasing the conductivity of solution. As a result, less energy was utilized to destruct organic pollutant and generate H_2O_2 and O_3 (as shown in Fig. S1). Table S3 shows that the conductivity of solution got a little increment after 20 min treatment owing to more charged fractions generated in solution. Compared with liquid discharge, different initial solution conductivities with the span of 17.4 μS/cm to 5.53 mS/cm expressed little effect on the decoloration of azo dye in this study [26].

3.4. Effect of initial pH

It is well known that the pH of the wastewater varies in a large span and the oxidation processes are very sensitive to the pH of the aqueous solutions [27]. The decoloration efficiency of aqueous MO with different initial pH was obtained and shown in Fig. 6. It is clear that when the solution pH was modified to 11.22, decoloration efficiency evidently dropped to 89.8%. The possible explanation for this result is that hydroxyl radicals can be scavenged by hydroxide ions [28]. The reaction between hydroxyl radicals and hydroxide ions is given as:

$$OH^{\cdot} + OH^{-} \rightarrow O^{\cdot -}H_2O \quad k = 1.3 \times 10^{10}(Ms)^{-1} \tag{16}$$

Plasma contains lots of active species such O_3^-, $OH^{\cdot}$,$O^{\cdot}$,O_3, Which have high oxidation potential in acid solution as represented in Table S4. Thus, by lowering the pH to 5.01 with hydrochloric acid, the efficiency was optimally 92.2%. Whereas, at pH 3.4 only 88.9% of the MO was removed. The possible reason is that the pH of MO solution not only affected the activity of some species contained in the liquid, but also affected the characteristics of the dye micelle. It is known that MO is an acid–base indicator and its color alter interval is pH 3.1–4.4 [29]. MO molecules can be partially monoprotonated to quinoid at pH 3.4, depicted in Eq. (17), which is more stable than azo form [30]. Therefore, the strong acidic condition blocked MO degradation.

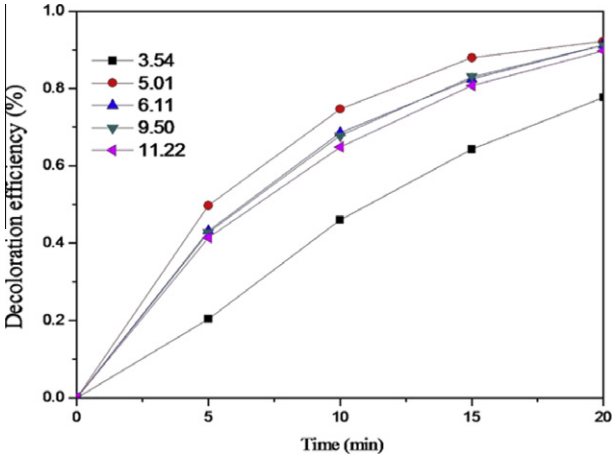

Fig. 6. Effect of solution pH on MO degradation (conditions: input energy 5.67 W; total volume 400 mL; initial concentration 60 mg/L; gas velocity rate 0.06 m^3/h; treatment time 20 min; virgin pH 6.10).

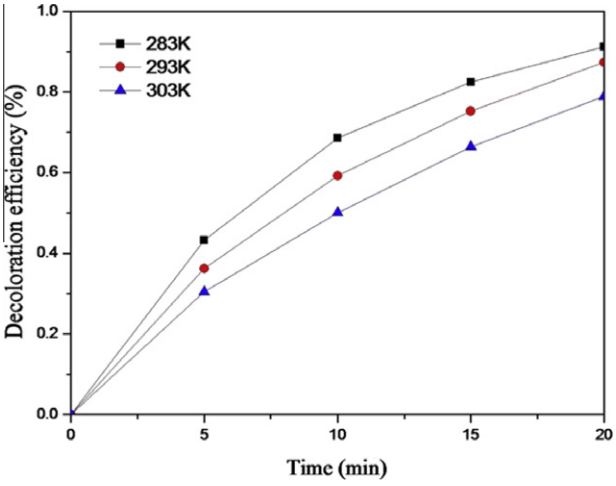

Fig. 7. Effect of temperature on MO degradation (conditions: input energy 5.67 W; total volume 400 mL; initial concentration 60 mg/L; gas velocity rate 0.06 m^3/h; treatment time 20 min).

the concentration and the live time of radicals were two main factors influencing the decoloration efficiency. And high temperature

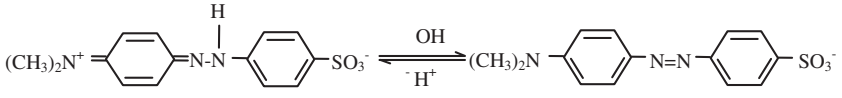

red (quinoid) yellow (azo) (17)

3.5. Effect of temperature

High temperature favored the dissociation of H_2O, which implies that more oxidative species can be produced and organic removal efficiently may rise with temperature increasing within a certain range [31,32]. However, in this case as presented in Fig. 7, the decoloration efficiency and rate constant reduced from 91% to 79% and from 0.119 min^{-1} to 0.075 min^{-1}, respectively, at the temperature from 283 K to 303 K. Gao et al. [33] proposed that

led to quenching hydroxyl radical and shortening life span of radical. Above, we may conclude that the negative effect of temperature on MO degradation was higher than the positive effect, thus increasing temperature caused a decreasing degradation rate. The activation energy (E_a) of the reactions is obtained from the Arrhenius equation followed as:

$$k = k_0 \exp\left(\frac{-E_a}{RT}\right) \tag{18}$$

$$Ln\,k = Ln\,k_0 - \frac{E_a}{RT} \quad (19)$$

where k_0 and k are the frequency factor and reaction rate constant, respectively. T and R denote the absolute temperature and ideal gas constant (8.314 J/(mol K)), respectively. The function plot is displayed in Fig. S2 and the measured activation energy values for the degradation of MO was 16.42 kJ/mol (R = 0.975).

3.6. Efficiency comparison of different reactor system

To evaluate the energy efficiency improvement capacity of GDC, the efficiency of other three reactor systems were also tested in oxygen atmosphere in this study. The first prototype was designed as a batch reactor (BR) with needle–plate electrodes to generate spark discharge above the water reservoir. The second prototype was only liquid circulating system (OLC) with gas directly flowing outside from discharge reactor. Besides, experiment data of hybrid gas–liquid electrical discharge (GL) was from previous study [34]. The obtained results are shown in Fig. 8a, suggesting that their removal processes followed pseudo-first-order kinetics. As shown in Table 1, after plasma treatment, the rate constant for MO degradation in GDC (13.4×10^{-2} min^{-1}) was larger than the values obtained in OLC (7.7×10^{-2} min^{-1}) and in BR (2.6×10^{-2} min^{-1}). Furthermore, compared with OLC and BR, the energy efficiency of GDC enhanced 51.5% and 200.3%, respectively. In BR system, there was only plasma exerting influence on the surface of bulk solution with few active species diffusing into the bulk solution. However, with the liquid circulating designed into BR system, the rate constant got sharply increment from 2.6×10^{-2} to 7.7×10^{-2} min^{-1}. This can be ascribed to that much more fresh solution was directly exposure to plasma and more active species diffused into the solution as presented in Table 1. From the experiment data, the conclusion can be withdrawn that in GDC process, liquid circulating only contributed 57.5% for the MO degradation and the left can be assigned to the gas circulating. It has been proposed that hybrid gas–liquid electrical discharge (GL) displays better decoloration efficiency than gas discharge and liquid discharge [35]. However, the experimental data in Table 1 shows that GDC performed considerably much better than the GL degrading MO. It is confirmed that ozone and hydroxyl radicals are formed in the gas and hydrogen peroxide is produced in the liquid with high-voltage electrodes over the water surface and ground electrodes in the water [36–38]. Moreover, in GDC process, the hydroxyl radicals were produced directly by dissociation of water molecules and indirectly from ozone, water and UV photons and its production efficiency was high compared to GL with high-voltage electrode placed in the liquid-phase [39,40]. Above, compared with GL, synergistic effect of active gas circulating, liquid circulating and high productivity of active species were responsible for high MO removal efficiency in GDC process. Fig. 8b illustrates that for the four reactor systems (GDC, OLC, GL and BR), the COD removal increased to 67%, 58%, 39% and 58%, respectively.

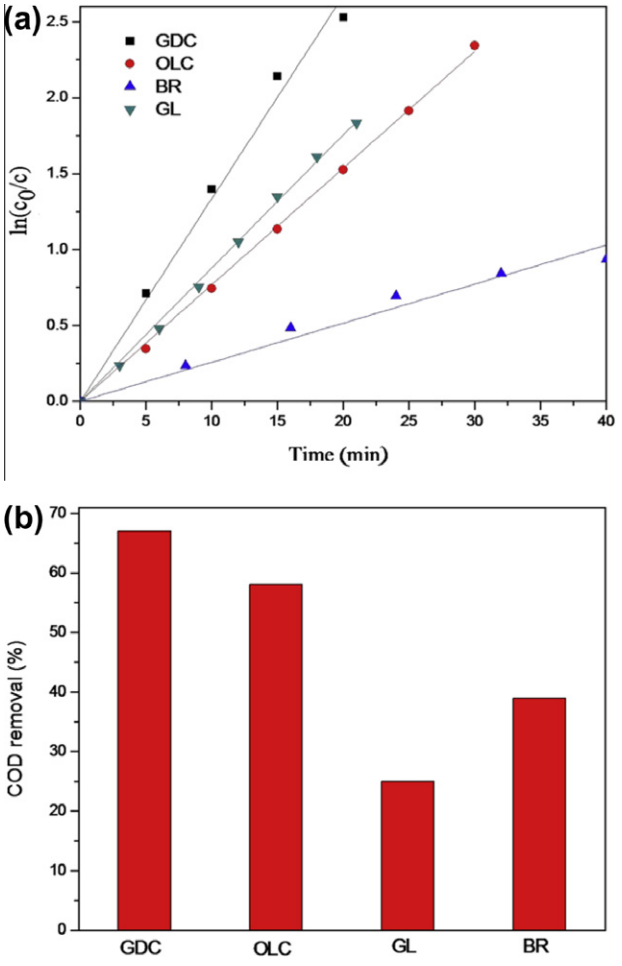

Fig. 8. (a) Rate constant comparison of different reactor systems, (b) COD removal comparison of different reactor systems (GDC, OLC and BR conditions: input energy 5.67 W; total volume 400 mL; initial concentration 60 mg/L; gas velocity rate 0.06 m^3/h; GL condition: input energy 7.09 W; total volume 200 mL; initial concentration 60 mg/L; gas velocity rate 0.12 m^3/h; temperature: 283 K).

Table 1
Comparison of energy efficiency and rate constant for the four electrical discharge processes.

Reactor system	Rate constant ($\times 10^{-2}$ min^{-1})	G(MO) (g/kW h)	G(H_2O_2) (g/kW h)	G(O_3) ($\times 10^{-3}$ g/kW h)
GDC	13.4	11.59	1.71	28.3
OLC	7.7	7.65	0.61	15.7
BR	2.6	3.86	0.57	4.8
GL	8.8	4.06	–	–

3.7. Presumption of degradation mechanism of MO

It has been well demonstrated that hydroxyl radical and O_3, etc. have high oxidation potential and efficiently attack the dye pollutants [41,42]. Therefore, in this reactor where the major degradation mechanism was likely hydroxyl radical and O_3, etc. attack. Based on bond dissociation energies (BDEs) theory, proposed pathways for the oxidation of MO by hydroxyl radical and ozone in GDC are represented in Fig. 9. When MO dissolved in aqueous solution, the weakest electrovalent bond (O_3S—Na) immediately dissociated. According to Table 2, the dissociation energies of C—S bonds in the groups $HOSO_2$—CH_3, H_3CSO_2—CH_3, and H_3CSO_2—C_6H_5 are about 77.5, 66.8, and 82.3 kcal/mol, respectively. It illustrates that compared with H_3CSO_2—C_6H_5, the intensity of C—S bonds is strengthened in $HOSO_2$—C_6H_5 and hence above 82.3 kcal/mol. Thus, the C—N—C bond dissociation energies is the lowest and the easiest to dissociate resulting in two demethylation reactions firstly taking place with plasma treatment. As presented in Table 2, bond energy for HN=NH double bonds is about 119.7 kcal/mol and larger than C_6H_5—$N_2C_6H_5$. Thus, C—N bond in the intermediate group (C_6H_5—$N_2C_6H_5$) is weak enough and can be easily cleaved by high-reactive species (O_3, OH·) produced by gas phase discharge. After treating for 30 min, the MO solution was analyzed by ion chromatography (as shown in Fig. S3). The ions SO_4^{2-} and NO_3^- were found, indicating that MO molecules and intermediate

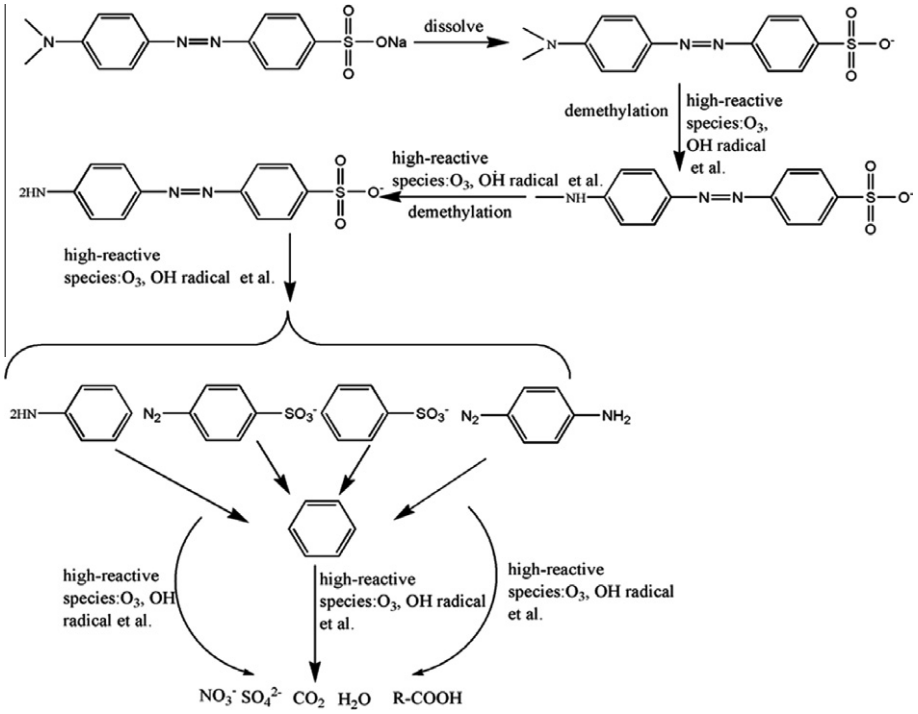

Fig. 9. Proposed pathways for the degradation of MO using non-thermal plasma.

Table 2
Datasheet of chemical bond dissociation energies [48].

Molecule bonds	Bond energy (kcal/mol)
C_6H_5—$N(CH_3)_2$	93.2 ± 2.5
CH_3—$N(CH_3)C_6H_5$	70.8
C_6H_5—$N_2C_6H_5$	82.3 ± 1.2
C_6H_5—$NHCH_3$	100.6 ± 2.5
HN=NH	119.7
$HOSO_2$—CH_3	77.5 ± 3
H_3CSO_2—CH_3	66.8
C_6H_5NH—CH_3	71.4 ± 2
H_3CSO_2—C_6H_5	82.3 ± 2

products were mineralized into CO_2, H_2O, SO_4^{2-} and NO_3^- during the plasma treatment process as depicted in Fig. 9.

In the realm of advanced oxidation processes (AOPs), some active species (i.e. O_3, OH·, etc.) as well as some physical effects (i.e. UV, ultrasonic, electrohydraulic cavitation, etc.) are responsible for organic degradation and can efficiently mineralized the organic molecules into harmless species [43–45]. In different systems for MO degradation, every mechanism proposed was specific due to different experiment systems and analytical methods. However, it was found that some analogous intermediates were detected in different degradation processes [46,47]. For example, the species of *m*/*z* 276 (after two demethylation reactions) and other intermediate products were found in photocatalytic degradation process, which were proposed in degradation mechanism in Fig. 9 based on bond dissociation energies (BDEs) theory [46].

4. Conclusions

GDC can effectively mineralize organic in aqueous solution and is a viable alternative for the treatment of refractory organic pollutants in view of fast removal rate and environmental friendliness. The degradation of MO by GDC followed pseudo-first order laws. In the experimental system, gas velocity, solution conductivity, temperature and pH of MO solution were all important factors for decoloration efficiency. The rise of initial concentration, volume and temperature caused the decrease of the apparent rate constant. And as gas velocity increased, more ozone was formed to react with MO in the reaction system. Besides, acceptable efficiency can be achieved in relatively large conductivity scale. Relatively high MO removal efficiency was obtained at medium pH solution. GDC process can efficiently mineralize the organic pollutant with 67% COD removal after 20 min treatment.

Acknowledgments

This work is financially supported by National Natural Science Foundation of China (Nos. 20776159, 21176260) and Natural Science Foundation of Shandong province (No. 09CX05009A).

Appendix A. Supplementary material

Supplementary data associated with this article can be found, in the online version, at http://dx.doi.org/10.1016/j.cej.2012.07.088.

References

[1] K. Dutta, S. Mukhopadhyay, S. Bhattacharjee, Chemical oxidation of methylene blue using Fenton-like reactions, J. Hazard. Mater. 84 (2001) 57–71.
[2] I.A. Salem, M.S. El-Maazawi, Kinetics and mechanism of color removal of methylene blue with hydrogen peroxide catalyzed by some supported alumina surfaces, Chemosphere 41 (2000) 1173–1180.
[3] P. Jantawasu, T. Sreethawong, S. Chavadej, Photocatalytic activity of nanocrystalline mesoporous-assembled TiO_2 photocatalyst for degradation of methyl orange monoazo dye in aqueous wastewater, Chem. Eng. J. 155 (2009) 223–233.
[4] M.S. Lucas, J.A. Peres, Decolorization of the azo dye Reactive Black 5 by Fenton and photo-Fenton oxidation, Dyes Pigments 71 (2006) 236–244.
[5] S. Haji, B. Benstaali, N. Al-Bastaki, Degradation of methyl orange by UV/H_2O_2 advanced oxidation process, Chem. Eng. J. 168 (2011) 134–139.
[6] M. Magureanu, D. Piroi, N.B. Mandache, Degradation of antibiotics in water by non-thermal plasma treatment, Water Res. 45 (2011) 3407–3416.
[7] A.A. Joshi, B.R. Locke, P. Arce, Formation of hydroxyl radicals, hydrogen peroxide and aqueous electrons by pulsed streamer corona discharge, J. Hazard. Mater. 41 (1995) 3–30.

[8] B.R. Locke, M. Sato, Electrohydraulic discharge and nonthermal plasma for water treatment, Ind. Eng. Chem. Res. 45 (2006) 882–905.
[9] P. Lukes, M. Clupek, V. Babicky, Generation of ozone by pulsed corona discharge over water surface in hybrid gas–liquid electrical discharge reactor, J. Phys. D: Appl. Phys. 38 (2005) 409–416.
[10] E. Njoyim, P. Ghogomu, S. Laminsi, Coupling gliding discharge treatment and catalysis by oyster shell powder for pollution abatement of surface waters, Ind. Eng. Chem. Res. 48 (2009) 9773–9780.
[11] A. Bogaerts, E. Neyts, R. Gijbels, Gas discharge plasmas and their applications, Spectrochim. Acta B 57 (2002) 609–658.
[12] H. Krause, B. Schweiger, J. Schuhmacher, Degradation of the endocrine disrupting chemicals (EDCs) carbamazepine, clofibric acid, and iopromide by corona discharge over water, Chemosphere 75 (2009) 163–168.
[13] H. Bader, J. Hoigne, Determination of ozone in water by the indigo method, Water Res. 15 (1981) 449–456.
[14] R.M. Selles, Spectrophotometric determination of hydrogen peroxide using potassium titanium(IV) oxalate, Analyst 105 (1980) 950–954.
[15] M. Kornaros, G. Lyberatos, Biological treatment of wastewaters from a dye manufacturing company using a trickling filter, J. Hazard. Mater. 136 (2006) 95–102.
[16] A.L. Ahmada, S.W. Puasab, M.M.D. Zulkali, Micellar-enhanced ultrafiltration for removal of reactive dyes from an aqueous solution, Desalination 191 (2006) 153–161.
[17] F. Banat, N. Al-Bastaki, Treating dye wastewater by an integrated process of adsorption using activated carbon and ultrafiltration, Desalination 170 (2004) 69–75.
[18] E. Haque, J.W. Jun, S.H. Jhung, Adsorptive removal of methyl orange and methylene blue from aqueous solution with a metal–organic framework material, iron terephthalate (MOF-235), J. Hazard. Mater. 185 (2011) 507–511.
[19] K.P. Singh, D. Mohan, S. Sinha, Color removal from wastewater using low-cost activated carbon derived from agricultural waste material, Ind. Eng. Chem. Res. 42 (2003) 1965–1976.
[20] A. Szygu1a, E. Guibal, M.A. Palacın, Removal of an anionic dye (Acid Blue 92) by coagulation–flocculation using chitosan, J. Environ. Manage. 90 (2009) 2979–2986.
[21] Y. Liu, D.Z. Sun, Development of Fe_2O_3–CeO_2–TiO_2/γ-Al_2O_3 as catalyst for catalytic wet air oxidation of methyl orange azo dye under room condition, Appl. Catal. B: Environ. 72 (2007) 205–211.
[22] S.J. Zhang, H.Q. Yu, Q.R. Li, Radiolytic degradation of Acid Orange 7: a mechanistic study, Chemosphere 61 (2005) 1003–1011.
[23] I. Grčić, S. Papić, K. Žižek, Zero-valent iron (ZVI) Fenton oxidation of reactive dye wastewater under UV-C and solar irradiation, Chem. Eng. J. 195–196 (2012) 77–90.
[24] J.H. Chen, J.H. Davidson, Ozone production in the negative DC corona: the dependence of discharge polarity, Plasma Chem. Plasma Process. 23 (2003) 501–518.
[25] J.W. Feng, Z. Zheng, J.F. Luan, Gas–liquid hybrid discharge-induced degradation of diuron in aqueous solution, J. Hazard. Mater. 164 (2009) 838–846.
[26] H.J. Wang, J. Li, X. Quan, Decoloration of azo dye by a multi-needle-to-plate high-voltage pulsed corona discharge system in water, J. Electrostat. 64 (2006) 416–421.
[27] S.F. Kang, C.H. Liao, S.T. Po, Decolorization of textile wastewater by photo-Fenton oxidation technology, Chemosphere 41 (2000) 1287–1294.
[28] M. Sahni, Analysis of Chemical Reactions in Pulsed Streamer Discharges: An Experimental Study. Ph.D. Thesis, Florida State University, 2006.
[29] N. Barka, A. Assabbane, A. Nounah, Photocatalytic degradation of methyl orange with immobilized TiO_2 nanoparticles: effect of pH and some inorganic anions, Phys. Chem. News 41 (2008) 85–88.
[30] J. Guo, Y.Y. Du, Y.Q. Lan, Photodegradation mechanism and kinetics of methyl orange catalyzed by Fe(III) and citric acid, J. Hazard. Mater. 186 (2011) 2083–2088.
[31] B. Ruscic, D. Feller, D.A. Dixon, Evidence for a lower enthalpy of formation of hydroxyl radical and a lower gas-phase bond dissociation energy of water, J. Phys. Chem. A 105 (2001) 1–4.
[32] B. Ruscic, A.F. Wagner, L.B. Harding, On the enthalpy of formation of hydroxyl radical and gas-phase bond dissociation energies of water and hydroxyl, J. Phys. Chem. A 106 (2002) 2727–2747.
[33] J.Z. Gao, X.Y. Wang, Z.G. Hu, H.L. Deng, J.G. Hou, X.G. Lu, J.W. Kang, Plasma degradation of dyes in water with contact glow discharge electrolysis, Water Res. 37 (2003) 267–272.
[34] Y.Z. Zhang, J.T. Zheng, X.F. Qu, Effect of granular activated carbon on degradation of methyl orange when applied in combination with high-voltage pulse discharge, J. Colloid Interface Sci. 316 (2007) 523–530.
[35] M. Sahni, B.R. Locke, Degradation of chemical warfare agent simulants using gas–liquid pulsed streamer discharges, J. Hazard. Mater. B 137 (2006) 1025–1034.
[36] I.M. Piskarev, Choice of conditions of an electrical discharge for generating chemically active particles for the decomposition of impurities in water, Technol. Phys. 44 (1999) 53–58.
[37] N.A. Aristova, I.M. Piskarev, Characteristic features of reactions initiated by a flash corona discharge, Technol. Phys. 47 (2002) 1246–1249.
[38] I.M. Piskarev, A.E. Rylova, A.I. Sevastyanov, Formation of ozone and hydrogen peroxide during an electrical discharge in the solution gas system, Russ. J. Electrochem. 32 (1996) 827–829.
[39] W. Hoeben, E. Veldhuizen, W. Rutgers, C. Cramers, G. Kroesen, The degradation of aqueous phenol solutions by pulsed positive corona discharges, Plasma Sources Sci. Technol. 9 (2000) 361–369.
[40] W. Hoeben, Pulsed Corona-Induced Degradation of Organic Materials in Water. Ph.D. Thesis. Eindhoven University of Technology, 2000.
[41] H. Zhang, J.L. Duan, D.B. Zhang, Decolorization of methyl orange by ozonation in combination with ultrasonic irradiation, J. Hazard. Mater. B 138 (2006) 53–59.
[42] L.C.Y. Chen, Effects of factors and interaction factors on the optimal decolorization process of methyl orange by ozone, Water Res. 34 (2000) 974–982.
[43] F.M. Huang, C. Li, H.L. Wang, Z.C. Yan, Analysis of the degradation mechanism of methylene blue by atmospheric pressure dielectric barrier discharge plasma, Chem. Eng. J. 162 (2010) 250–256.
[44] A.B. Mohamed, A.M. Sawsan, F.M. Mohamed, One-pot template synthesis of Ti–Al-containing mesoporous silicas and their application as potential photocatalytic degradation of chlorophenols, Appl. Catal. B: Environ. 107 (2011) 316–326.
[45] J. Wang, B.D. Guo, X.D. Zhang, Sonocatalytic degradation of methyl orange in the presence of TiO_2 catalysts and catalytic activity comparison of rutile and anatase, Ultrason. Sonochem. 12 (2005) 331–337.
[46] C. Baiocchi, M.C. Brussino, E. Pramauro, Characterization of methyl orange and its photocatalytic degradation products by HPLC/UV–VIS diode array and atmospheric pressure ionization quadrupole ion trap mass spectrometry, Int. J. Mass Spectrom. 214 (2002) 247–256.
[47] L. Gomathi Devi, S. Girish Kumar, K. Mohan Reddy, Photo degradation of methyl orange an azo dye by advanced fenton process using zero valent metallic iron: influence of various reaction parameters and its degradation mechanism, J. Hazard. Mater. 164 (2009) 459–467.
[48] Y.R. Luo, Handbook of Bond Dissociation Energies in Organic Compounds, Science Press, Beijing, 2005.